

Sensitivity of an Ocean Model to “Details” of Stochastic Forcing

Cécile Penland and Philip Sura

NOAA-CIRES/Climate Diagnostics Center, Boulder CO 80305-3328

Abstract

We review the sensitivity of a double-gyre ocean model to various stochastic versions of parameterization representing unresolved, rapidly-varying atmospheric wind forcing. Although each version can be argued to be a valid representation of a single physical process and, therefore, may be expected to excite the model in ways similar to the other versions, the model response is surprisingly variable with respect to the details of the parameterization method.

1. Introduction

The idea of “just shaking the model a little” in order to see how the “important” dynamics behave has been around for a long time. Unfortunately, it has been shown (e.g., Sura and Penland 2002) that there is no such thing as “just” shaking it a “little.” Deterministic and stochastic dynamics in a numerical model generally combine in such a way that the implementation method of each is important. Further, the volatile nature of stochasticity can render the statistics of model output even more sensitive to the implementation details of the random forcing than to details of the deterministic formulation.

We explore these ideas in the context of the double-gyre ocean model used by Sura et al. (2001) to study the oceanic circulation response to additive, stochastic forcing. Their study was primarily concerned with the interannual and interdecadal time scales found in the monthly-averaged output of this model. Since the size of the model time step (20 minutes) compared with the time scales of interest was so small, it seemed reasonable that coupling the ocean model with the stochastic atmosphere might be safely performed once per day rather than every time step, and this is what they did. Similar reasoning suggests that the exact nature of the temporal correlation (i.e., constant forcing changed abruptly every day vs. an exponential decay with a correlation time of one day) would be unimportant on monthly to interdecadal time scales.

Another consideration is how the distribution of random forcing might affect the model output statistics. Compare a flat distribution of sample forces confined between finite boundaries to a Gaussian distribution with the same variance as the flat one. The Gaussian distribution has its largest values around zero, and so one might expect the flat distribution to engender more variability in the model than the Gaussian. However, the Gaussian distribution has tails extending to infinity, and so someone else might expect the flat distribution to engender less variability than the Gaussian. A third investigator might think that the model output from one case would be very similar to that of the other since both distributions have the same variance.

Sura and Penland (2002) have investigated these questions in some detail and their results are summarized below.

2. Model and Experimental Setup

The nonlinear reduced-gravity equations in transport form are used to model the upper ocean in a rectangular basin of 2400 km by 2400 km extent; (x, y) -coordinates increasing eastward and northward are used. The details of the model are to be found in Sura et al. (2001) and in Sura and Penland (2002). The ocean model is driven by the wind stress, which consists of a mean component and a stochastic component. The mean wind stress is represented by a zonal wind field with a sinusoidal pattern, which generates a northern, cyclonic, subpolar gyre and a southern, anticyclonic, subtropical gyre. The spatially inhomogeneous stochastic forcing accounts for the mid-latitude synoptic atmospheric variability and is parameterized by the bulk formula for the wind stress:

$$\tau_{stochastic} = \rho_{Air} C_D |\mathbf{u}'| \mathbf{u}'$$

$$u'(x, y, t) = \eta_x(t) f(x, y)$$

$$v'(x, y, t) = \eta_y(t) f(x, y),$$

where ρ_{Air} , $|\mathbf{u}'|$ and \mathbf{u}' are the air density (1.3 kg m^{-3}), near surface wind speed, and velocity; C_D (2×10^{-3}) is the drag coefficient, and $\eta_{x,y}(t)$ are independent stochastic processes with zero mean and standard deviation σ . The weight function $f(x, y)$ parameterizes the spatial structure of the atmospheric variability by a Gaussian shape with circular symmetry, a standard deviation of 600 km, and origin placed in the center of the basin. Of course, we are mostly interested in the properties of $\eta_{x,y}(t)$.

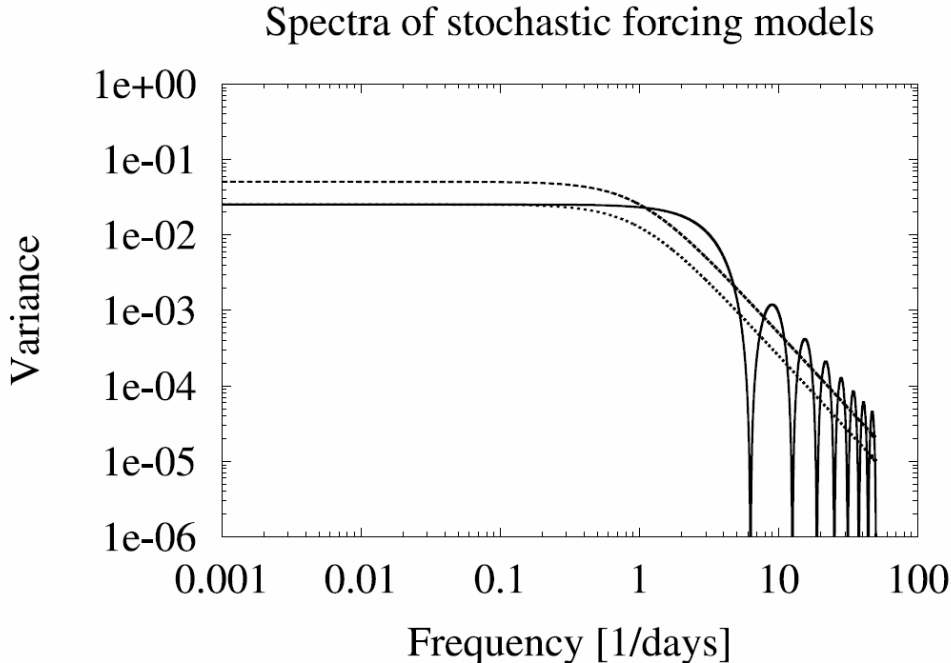


Figure 1: Spectra of stochastic forcing. Solid line: Models 1 and 2. Dashed line: Model 3. Dotted line: Model 4.

Four forms of stochastic driving are considered. The first (Model 1) is that of Sura et al. (2000, 2001), who sampled a flat distribution. For a flat distribution with zero mean and variance $\sigma^2 = (2\eta_o)^2/12$, the probability density is constant in the interval $(-\eta_o, \eta_o)$. The noise is updated once per day. The forcing in

the second experiment (Model 2) is also sampled once daily, but from a Gaussian probability distribution. The third experiment (Model 3) consists of forcing the ocean model with Gaussian red noise having a decay time of 1 day, but sampled at each 20-minute time step during the model integration. Thus, the autocorrelation function for the forcing in Models 1 and 2 is equal to unity for lags less than one day and equal to zero for greater lags. The autocorrelation function for the stochastic forcing in Model 3 decays exponentially with an e-folding time of one day. Models 2 and 3 are constructed so that their Gaussian distribution has the same variance as the flat distribution of Model 1. The spectra of the different stochastic models are shown in Fig. 1.

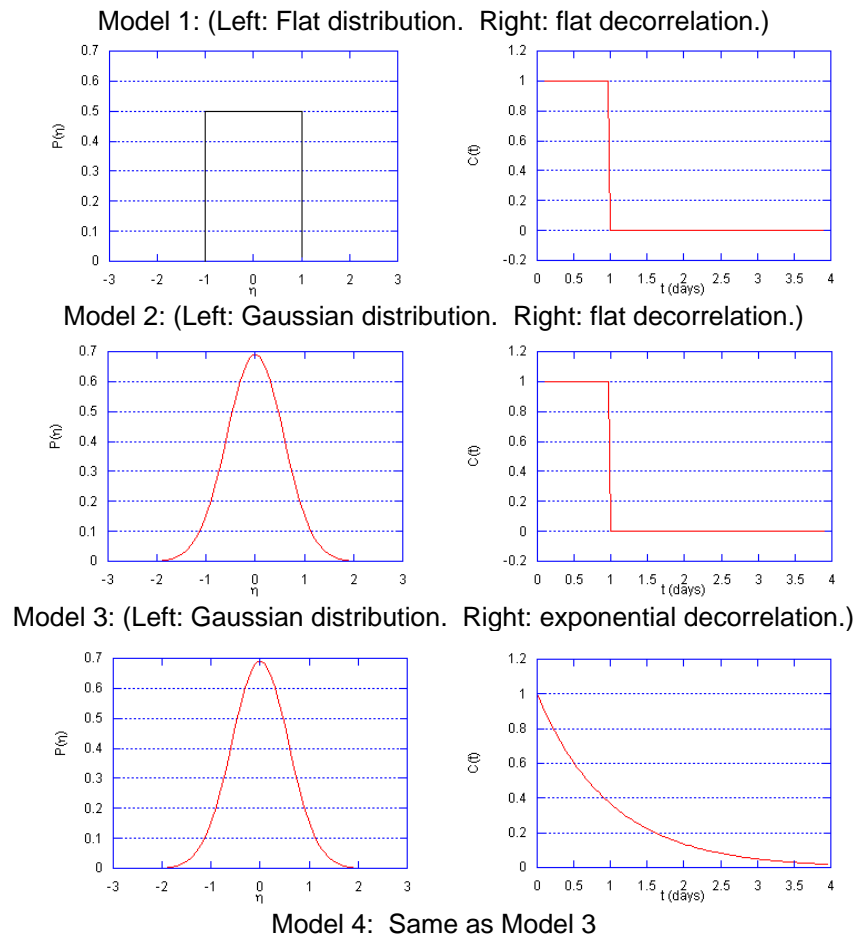


Figure 2: Distributions (left) and autocorrelation functions (right) of Models 1-4.

Because Model 3 has a higher variability above the e-folding timescale of one day than the spectra of Models 1 and 2, a fourth experiment (Model 4), similar to Model 3, but with the low-frequency part of the spectrum coinciding with the spectra of Models 1 and 2. The total variance of Model 4’s stochastic forcing is thus less than that of the others. The distribution and correlation properties of these models are summarized in Fig. 2.

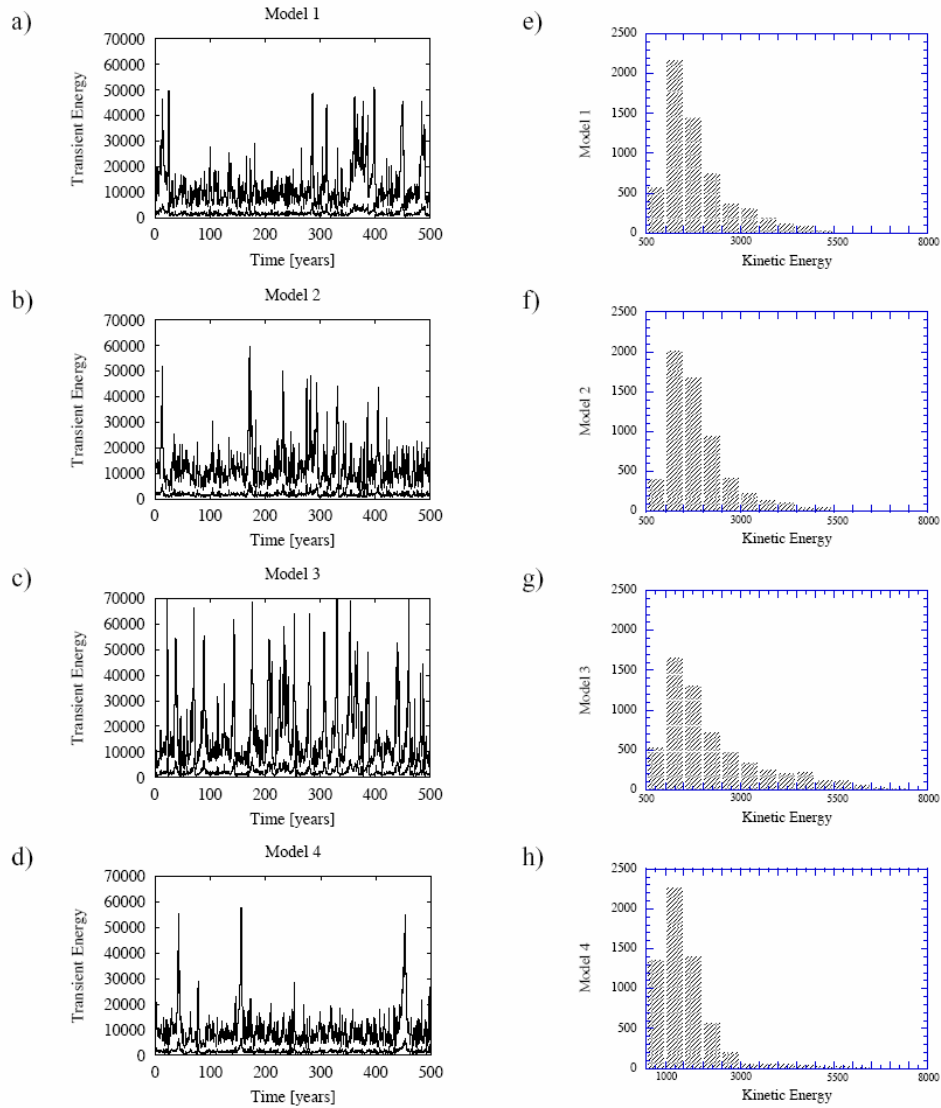


Figure 3: Time series (left) and histograms (right) of transient kinetic energy from the double-gyre ocean model driven by each of the four stochastic parameterizations.

3. Results

Time series and histograms of transient kinetic energy (TKE) of the oceanic circulation as estimated from the monthly-averaged output by all four models are shown in Fig. 3. Obviously, the differences are significant. We quantify the differences by classifying the TKE into three model-independent states: below normal, normal and above normal. The boundaries between these states happen to coincide with the boundaries of the TKE terciles for the control run (Model 1), but the range of “normal” for the other models is the same as that of Model 1.

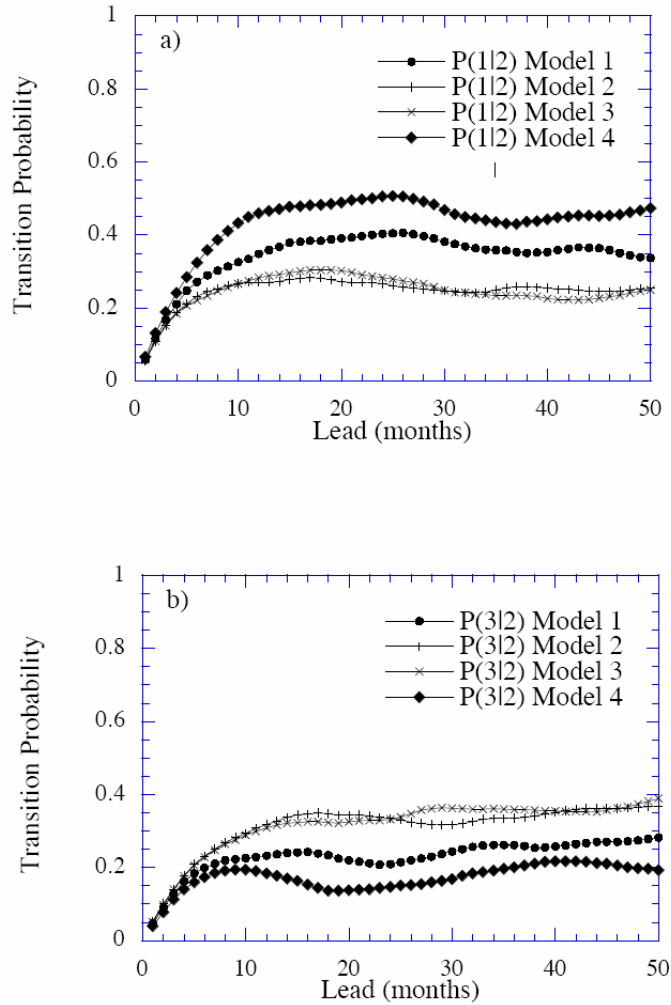


Figure 4: Probability of transition from “normal” transient kinetic energy state to (top) “below normal” state and to (bottom) “above normal” state.

The transition probability $p(i|j)$ of being in state i at some lead time later than it was known to be in state j is shown in Fig. 4. In this figure, the states $\{i = 1,2,3\}$ correspond, respectively, to being in the below normal, normal or normal state. Similarly, the recurrence probability $p(i|i)$ is shown in Fig. 5. These figures show the propensity of Model 4 to go into the lowest TKE state and stay there, consistent with the smallest amount of energy being applied to the system. Fig. 4 suggests that the distribution of the random forcing is more important to the probability of making a transition out of the normal TKE state than is the spectrum. In contrast, Fig. 5 suggests that the spectrum plays a greater role in the probability of recurrence than does the distribution.

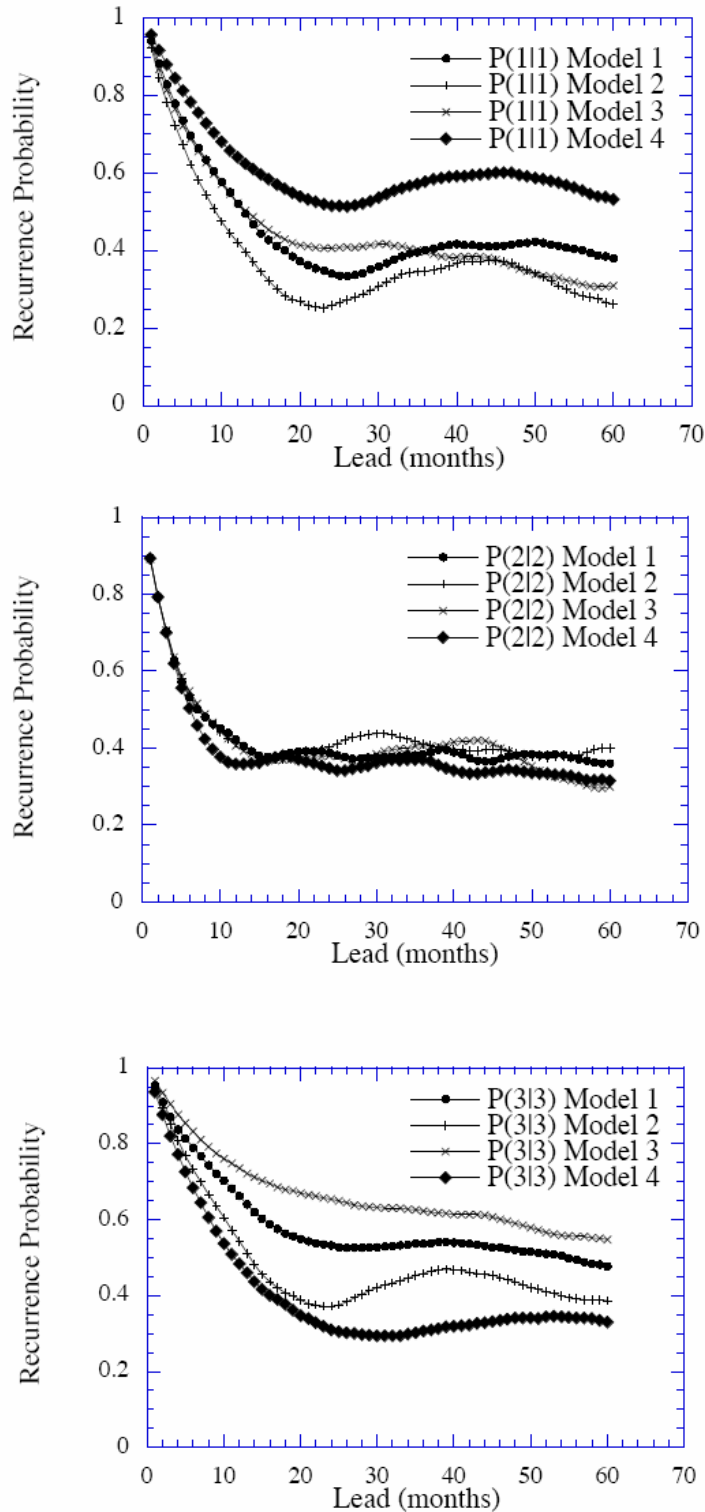


Figure 5: Recurrence probability as a function of lead time for (top) the “below normal,” (center) “normal,” and (bottom) “above normal” kinetic energy states.

4. Conclusions

Details of the forcing at short timescales affect long timescales. In spite of the fact that the models of stochastic forcing differed on timescales of 20 minutes to one day, these differences played a large role in the behavior of the monthly averaged data. Not only the spectrum of the stochastic forcing, but also the

distribution of the stochastic forcing, played a large role in the ocean model response. Our results imply that the tails of the Gaussian distribution excite more variability in the oceanic model than the peak of the distribution around zero suppresses it relative to variability excited by a flat distribution with the same variance. Choice of a stochastic parameterization model should therefore be based on physical and mathematical principles, such as the Central Limit Theorem (e.g., Khasminski 1966; Papanicolaou and Kohler 1974) as well as careful statistical analysis of data.

Acknowledgements: We would like to thank Klaus Fraedrich for helpful discussions and support. Part of this work and a visit of CP to Hamburg was supported by the Deutsche Forschungsgemeinschaft within Sonderforschungsbereich 512. Additional support by the Office of Naval Research and by the NASA Ocean Vector Science Team (JPL) is gratefully acknowledged.

5. References

- Khasminskii, R. Z., 1966: A limit theorem for the solutions of differential-equations with random right hand side. *Theory Probab. Appl.*, **11**, 390–406
- Kohler, W., Papanicolaou, G., 1977. Wave propagation in a randomly inhomogeneous ocean. In: Keller, J., and Papadakis, J. (Eds.), *Springer Lecture Notes in Physics*, vol. **10**. Springer, Berlin.
- Sura, P., Lunkeit, F., Fraedrich, K., 2000. Decadal variability in a simplified wind-driven ocean model. *J. Phys. Oceanogr.*, **30**, 1917–1930.
- Sura, P., Fraedrich, K., Lunkeit, F., 2001. Regime transitions in a stochastically forced double-gyre model. *J. Phys. Oceanogr.* **31**, 411–426.
- Sura, P., and C. Penland, 2002: Sensitivity of a double-gyre ocean model to details of stochastic forcing. *Ocean Modelling*, **4**, 327-345.

